J. Membrane Biol. 74, 103–113 (1983)

The Journal of
Membrane Biology

Junctional Transfer in Cultured Vascular Endothelium: I. Electrical Coupling

David M. Larson*, Ephraim Y. Kam and Judson D. Sheridan
Zoology Program and Department of Anatomy, University of Minnesota, Minneapolis, Minnesota 55455

Summary. Vascular endothelial cultures are composed of flat, polygonal monolayer cells which retain many of the growth, metabolic and physiological characteristics of the intimal endothelium. However, intercellular gap and tight junctions, which are thought to perform important roles in normal intimal physiology, are reduced in complexity and extent in culture. We have used electrophysiological techniques to test confluent (3- to 5-day) primary cultures of calf aortic (BAEC) and umbilical cord vein (BVEC) endothelium for junctional transfer of small ions. Both cell types are extensively electrically coupled. The passive electrical properties of the cultured cells were calculated from the decrease in induced membrane potential deflections with distance from an intracellular, hyperpolarizing electrode. Data analyses were based on a thin-sheet model for current flow (Bessel function). The generalized space constants (λ) were 208.6 μm (BAEC) and 288.9 μm (BVEC). The nonjunctional (6.14 and $8.72 \times 10^8\ \Omega$) and junctional (3.67 and $3.60 \times 10^6\ \Omega$) resistances were similar for the BAEC and BVEC, respectively. We detected no statistically significant differences in the resistance estimates for the two cell types. *In vivo* ultrastructural studies have suggested that aortic endothelium has more extensive gap junctions than venous endothelium. We have found that these ultrastructural differences are reduced in culture. The lack of any significant difference in electrical coupling capability suggests that cultured BAEC and BVEC have functionally similar junctional characteristics.

Key Words electrical coupling · vascular endothelium · gap junctions · culture · thin-sheet model · Bessel function

Introduction

Vascular endothelial cultures have become popular models for the intima of large blood vessels, due primarily to the fidelity of retention of *in vivo* biochemical, physiological, and growth characteristics in the culture dish (Jaffe, Hoyer & Nachman, 1973; Buonassisi & Venter, 1976; Gimbrone, 1976; D'Amore & Shepro, 1977; Schwartz, 1978; Mason et al., 1979; Buonassisi & Colburn, 1980). *In vivo*, endothelial cells demonstrate characteristic patterns of gap and tight junctions (Simionescu, Simionescu & Palade, 1975, 1976; Larson & Sheridan, 1982) throughout the vascular tree. According to the most complete study of endothelial junction distribution *in situ* (summarized in Simionescu & Simionescu, 1977), arteries and veins have different patterns of junctions with arterial endothelium having the larger and more frequent gap junctions. Ultrastructural studies on cultured aortic and venous endothelial cells have demonstrated the presence of gap and tight junctions, though reduced in extent and complexity (Larson & Sheridan, 1982). We have already reported (Larson & Sheridan, 1982) on the qualitative ability of the cultured cells to exchange small molecules, presumably by way of gap junctions (for reviews *see* McNutt & Weinstein, 1973; Hooper & Subak-Sharpe, 1981). The present study is a more quantitative analysis of junctional transfer utilizing electrophysiological measurements and a thin-sheet or two-dimensional cable model (Woodbury & Crill, 1961; Hyde et al., 1969; Shiba, 1971; Shiba & Kanno, 1971; Jongsma & van Rijn, 1972; Siegenbeek van Heukelom, Denier van der Gon & Prop, 1972). This model approximates the monolayer with an "infinite," thin, planar core conductor with parallel (upper and lower) high resistance plates. Intracellularly injected current is assumed to flow, from a point or cylindrical source, radially down the cytoplasmic and junctional resistivities and at right angles across the relatively high resistance of the nonjunctional plasma membranes.

Using this model, we have derived estimates of junctional and nonjunctional resistances for primary cultures of endothelial cells from calf

* *Present address:* Vascular Pathophysiology Laboratory, Department of Pathology; Brigham and Women's Hospital and Harvard Medical School, Boston, Massachusetts.

aortae and fetal calf umbilical cord veins. We have applied some new modifications of the fitting procedures to improve their reliability and have developed appropriate statistical methods (*see* Appendix) for the fitting and estimation techniques. A brief report on some of this work has appeared elsewhere (Larson & Sheridan, 1979).

Symbols:

$V_{r,\infty}$	= steady-state membrane potential deflection at distance r
i_o	= current injected
y_r	= transfer resistance $= V_{r,\infty}/i_o$
n	$= \rho_i/2\pi d$
$K_v(z)$	= modified Bessel function of the second kind (order $= v$; argument $= z$)
ρ_i	= resistivity of cytoplasm plus intercellular pathway
ρ_c	= resistivity of cytoplasm
R_j	= specific junctional resistance
r_j	= junctional resistance
$r_{j,1}$	= junctional resistance of one interface
R_m	= specific nonjunctional resistance
r_m	= nonjunctional resistance
r	= interelectrode distance (radial distance)
λ	= space constant $(=(R_m d/2\rho_i)^{1/2})$
d	= thickness of the monolayer
l	= length of one side of a model hexagonal cell
ω	= diameter of a cell (= internuclear distance)
X	= number of data points

Materials and Methods

Cell Culture

Endothelial cells were obtained from calf (*Bos taurus*) thoracic aortae and fetal calf umbilical cord veins by collagenase digestion (Booyse, Sedlak & Rafelson, 1975; Macarak, Howard & Kefalides, 1977; Larson & Sheridan, 1982). The freshly isolated cells were plated on plastic tissue culture dishes (Falcon Plastics) at a density of 5 to 7 $\times 10^5$ cells per 60 mm dish. The cultures were maintained at 37 °C in a humidified atmosphere at 95% air/5% CO_2 in Medium 199 (GIBCO), with 30% heat-inactivated calf serum (GIBCO), L-glutamine, and antibiotics (Larson & Sheridan, 1982). The culture medium was changed after 24 hr and then every other day until the cultures became confluent (3 to 5 days).

The cells were identified as endothelial primarily on the basis of morphology with confirmation by occasional parallel testing by indirect immunofluorescent staining for Factor VIII-associated protein (Jaffe et al., 1973; *data not shown*). The polygonal "cobblestone" morphology reported for endothelial cultures under similar growth conditions (Gimbrone, Cotran & Falkman, 1974; Booyse et al., 1975; Haudenschild et al., 1975; Ryan et al., 1978; Schwartz, 1978) was characteristic of our cultures (Fig. 1*A*). The problem of occasional and minor smooth muscle cell contamination was avoided by testing the cultures only in areas of cellular homogeneity.

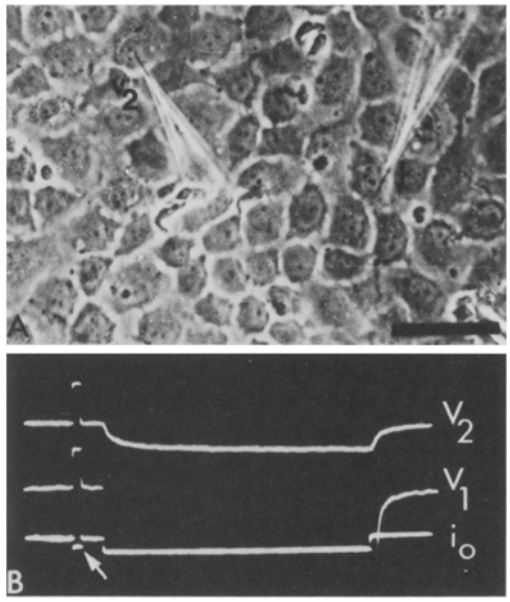

Fig. 1. Electrical coupling in an umbilical vein endothelial culture. (*A*) Phase-contrast micrograph (j = current-injecting electrode; v_2 = voltage-recording electrode; bar = 40 μm). (*B*) Oscilloscope tracings corresponding to (*A*) (i_o = current trace from j; V_1 = voltage trace from j; V_2 = voltage trace from v_2; current calibration pulse (arrow) $= 1 \times 10^{-9}$ amp; voltage calibration pulse $= 1 \times 10^{-3}$ volts)

Equipment

Current-injecting and voltage-recording electrodes were glass micropipettes prepared with a horizontal puller from Omega Dot capillary tubing. These micropipettes were filled with 3 M KCl/0.1 M K-acetate by the fiber-fill method (Tasaki et al., 1968) and connected to the amplifier circuit by Ag/AgCl wires. The microelectrodes had tip resistances of 5 to 8×10^7 Ohms, in medium, against the Ag/AgCl wire bath (indifferent) electrode.

Bridge circuits in the amplifiers allowed the monitoring of membrane potentials through the same electrodes used for injecting current.

Current pulses and membrane potential traces were displayed simultaneously on a four-channel oscilloscope. Calibration pulses for current and voltage traces were produced by a calibrator which also provided a virtual ground. Microelectrodes were mounted on micromanipulators arranged around the inverted microscope. All penetrations were observed under phase-contrast optics at 160×.

Protocol

All experiments were carried out at room temperature and atmosphere in standard growth medium. The cultures were allowed to equilibrate to these conditions and the experiments were continued for 45 to 90 min. The current-injecting electrode (j) was inserted into one cell (perinuclear) in the monolayer (Fig. 1). Another electrode (v_2), used for measuring membrane potential deflections, was inserted into another cell. Baseline membrane potential was monitored during each penetration and the cells were rejected if the measured potential was not maintained at

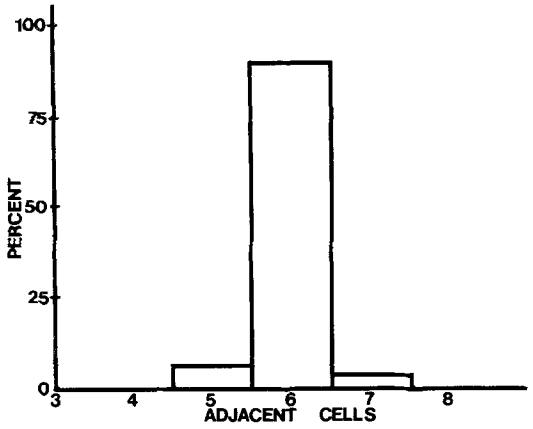

Fig. 2. Histogram describing the number of adjacent cells in phase micrographs of the cultures used for the electrical coupling experiments

-20 mV or greater (in order to insure minimal cellular damage). Rectangular hyperpolarizing current pulses of 1 to 5×10^{-9} amp and 100 to 300 msec duration were passed through electrode j and the consequent membrane potential deflections detected by electrode v_2 were recorded. Electrode v_2 was then removed and reinserted into another cell in the monolayer. In order to further minimize possible effects of cell damage, the sequence of penetration by v_2 was always from long interelectrode distances toward short, utilizing the full microscopic field. This procedure was followed until the stability of the cell with electrode j was impaired (1 to 7 penetrations with v_2). Both electrodes were then removed and the experiment was repeated on another area in the monolayer.

Data Collection

Oscilloscope tracings (Fig. 1) were recorded on linagraph film (Kodak RAR 2495) by means of an oscillographic camera. Several traces (at different current levels) were photographed during each penetration. In addition, phase micrographs were taken of each penetration in order to allow determination of interelectrode distance (r) (Fig. 1).

Current levels (i_0) and potential deflections ($V_{r,\infty}$) were measured by projection of the linagraph film and comparison with calibrator standards (*see* Fig. 1*B*). Only those traces in which the potential deflections reached steady state were used. A transfer resistance term was then calculated:

$$y_r = V_{r,\infty}/i_0.$$

Electrical coupling was operationally defined as the detection of a steady-state transfer resistance of at least 1×10^5 ohms. The average y_r was calculated for each pair of cells (2 to 8 traces at different current levels). The transfer resistance and interelectrode distance were used for quantitation of the characteristics of electrical coupling in these cultures.

Physical Dimensions of Cultured Endothelial Cells

By examination of phase micrographs of these experiments, it was determined that the endothelial cells had a mode of six adjacent cells (Fig. 2). Therefore, the cells were modeled as right hexagonal prisms. Using a hexagonal packing model (Larson, 1980), the average internuclear distance (ω) between adjacent cells was calculated for each experimental field and was assumed to be equal to the average cell diameter.

Since it proved impractical to examine the particular cells used above for estimation of cell thickness, thin sections (Larson & Sheridan, 1982), cut perpendicular to the dish, of glutaraldehyde-fixed, parallel cultures were used. The maximum lengths (diameters) and cross-sectional areas of cells cut through the nucleus were measured. The average thickness for each cell was obtained by dividing the area by the diameter. Linear regression (*not shown*; *see* Larson, 1980) of height on diameter allowed calculation of an average height (d) corresponding to the estimated diameters (ω) from the phase micrographs.

Results

Homogenous monolayers (Fig. 1) of 3 to 5-day-old aortic and umbilical vein endothelial cells were used for all experiments. For aortic cultures, 123 cell pairs were tested in 32 microscopic fields of 15 separate dishes from 11 different isolations. Ninety-four cell pairs from 42 fields of 16 dishes from 10 separate umbilical vein isolations were used. Under the experimental conditions employed (and even in most additional cases rejected due to low membrane potentials) coupling (Fig. 1*B*) was invariably detected at distances of 15 μm to over 300 μm. The average cell diameters, calculated from the phase micrographs, were 32.6 μm for aortic and 37.9 μm for umbilical vein cultures (*see* Table 1). The interpolated values for the thicknesses were 3.0 and 1.9 μm, respectively. Hence, coupling was detectable at least 10 cell diameters from the current-injecting electrode.

Quantitation of Electrotonic Transfer Characteristics

The combined data of transfer resistance and interelectrode distance $G(y_r, r)$, tabulated for aortic and umbilical vein cultures, were applied to the thin-sheet model using the formulation of Jongsma and van Rijn (1972).

The precise theoretical decline of induced membrane potential changes ($V_{r,\infty}$) with increasing interelectrode distance (r) is expressed by

$$V_{r,\infty} = n i_0 K_0(r/\lambda) \quad (1)$$

where n is a resistance term ($=\rho_i/2\pi d$), λ is the space constant, and $K_0(r/\lambda)$ is the zero order

Table 1. Physical dimension of cultured endothelial cells (ω = diameter; d = thickness; N = number of monolayers examined)

Cell type	N	$\omega \pm$ SD (10^{-4} cm)	$d^a \pm$ SD (10^{-4} cm)
Aortic	42	32.6± 9.3	3.0±(1.0)
Umbilical vein	42	37.9±10.4	1.9±(0.7)

[a] These thicknesses were determined by interpolation using regression lines from electron microscopic data (*see text*). Standard deviations were assumed to be equal to those for the electron microscopic data.

Bessel function of the modified second kind with (r/λ) as the argument.[1]

Since transfer resistance was used in the compilation of data:

$$y_r = V_{r,\infty}/i_o = nK_0(r/\lambda). \quad (2)$$

The use of the normalizing transfer resistance term was justified by the linear relationship between i_o and $V_{r,\infty}$ for given cell pairs. A typical current-voltage plot is shown in Fig. 3.

In order to find the n and λ which provide the best fit for the experimental data, a modified least-squares analysis was used (Jongsma & van Rijn, 1972). If S is the sum of the squared deviations from the theoretical curve, i.e.

$$S = \sum_G (y_r - nK_0(r/\lambda))^2, \quad (3)$$

then the best fitting n and λ can be found by setting the first partial differentials (with respect to n and λ) equal to zero and solving each equation for n (*see* Jongsma & van Rijn, 1972; their equations (A.5) and (A.6)). The smallest S and hence the best n and λ are found at the intersection of the resulting monotonically descending functions (e.g. Fig. A1 in the Appendix).

Due to the complexity of the Bessel functions, a computer program was generated to calculate the difference between the two values for n at given values for λ. This program on the Cyber 74 system at the University of Minnesota used a library program (Amos & Daniel, 1975) to calculate values for the Bessel functions. The iterative program found λ to the nearest 0.1 μm and then calculated the average n.

[1] Jongsma and van Rijn (1972) used the term "J_o" for current injected. Since this symbol (and I_o) also indicates a type of Bessel function, we have used "i_o" to avoid confusion.

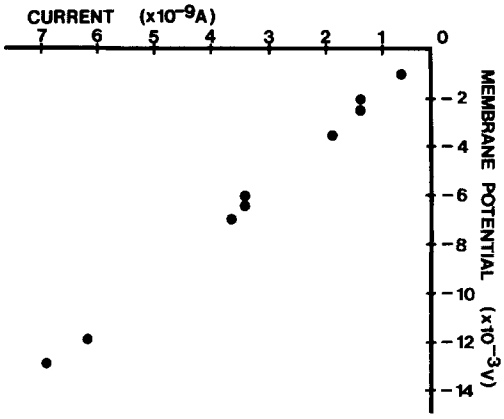

Fig. 3. Relationship between current-injected (nanoamperes) and membrane potential deflection recorded (millivolts) for a typical pair of cells at an interelectrode distance of 60 μm

The best fitting n and λ for the aortic (data set: AORTIC) and umbilical vein (data set: VEIN) monolayers are shown in Table 2. As can be seen, the calculated best estimates for these parameters are essentially the same in the two different preparations. The corresponding plots of the data sets and best fitting curves based on Eq. (2) are shown in Fig. 4*A* and *C*.

Logarithmic Transformation

As can be seen by examination of the plots of data sets AORTIC and VEIN in Fig. 4*A* and *C*, there is a much greater scatter of experimental points at short interelectrode distances than at longer distances. The use of the least-squares analysis requires the assumption of homoscedasticity of variances of the dependent variable (y_r) over the range of the independent variable (r) (Schmidt, 1975). This assumption is clearly unwarranted in these plots. In order to reduce this inconsistency, a natural logarithmic transformation was carried out.

The basic model equation (Eq. 2) therefore became

$$\ln y_r = \ln(nK_0(r/\lambda)), \quad (4)$$

and the least-squares equation became

$$S^* = \sum_G (\ln y_r - \ln n - \ln K_0(r/\lambda))^2. \quad (5)$$

Setting the first partial differentials of Eq. (5) equal to zero and solving each for n,

$$n_1 = \exp \frac{1}{X} \sum_G \ln \frac{y_r}{K_0(r/\lambda)}, \quad (6)$$

Table 2. Comparison of best-fitting parameters from Eq. (2) and (4) for all data sets and treatments

Data set	S	$n \pm$SD ($10^6\,\Omega$)	$\lambda \pm$SD (10^{-4} cm)	Covariance (n, λ)
Untransformed:				
AORTIC	1.483×10^{15}	3.66 ± 0.66	152.5 ± 36.6	-2267
VEIN	0.390×10^{15}	3.89 ± 0.59	159.2 ± 29.9	-1697
ln-Transformed:				
AORTIC	65.29	2.07 ± 0.25	208.6 ± 24.6	-576
VEIN	27.44	2.07 ± 0.25	288.9 ± 40.9	-975

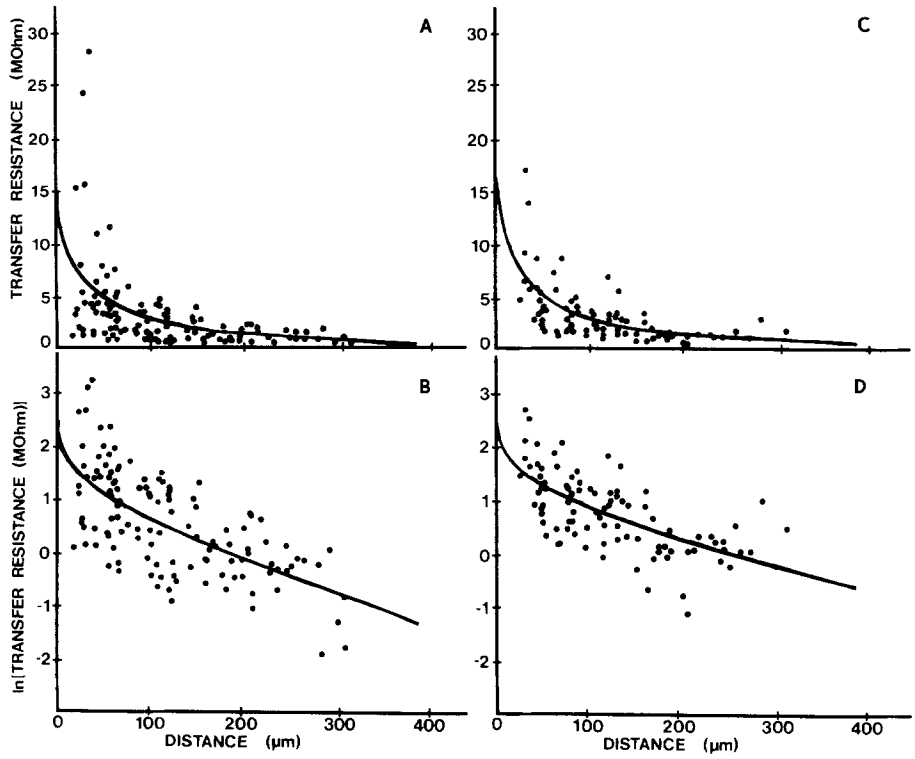

Fig. 4. Plots of transfer resistance (MΩ) versus interelectrode distance (μm) for cultured endothelial cells with the best fitting Bessel function curves. (*A*) Untransformed data set AORTIC with a curve based on Eq. (2). (*B*) Natural logarithm-transformed data set AORTIC (Eq. 4). (*C*) Untransformed data set VEIN (Eq. 2). (*D*) Natural logarithm-transformed data set VEIN (Eq. 4)

and

$$n_2 = \exp \frac{\sum_G r \left(\ln \frac{y_r}{K_0(r/\lambda)} \right) \frac{K_1(r/\lambda)}{K_0(r/\lambda)}}{\sum_G r \frac{K_1(r/\lambda)}{K_0(r/\lambda)}} \qquad (7)$$

where X is the number of experimental data points.

Calculation of the best n's and λ's were carried out with a computer program similar to that mentioned above. The new values for n and λ for each data set are listed in Table 2. As can be seen in the corresponding Fig. 4*B* and *D*, this transformation improved the apparent adherence of the data bases to the assumption of equal variance of y_r over the range of r.

Estimation of the Junctional and Nonjunctional Resistances

Junctional Resistance. The lumped intercellular and intracellular resistivity ρ_i was calculated from the resistance term n since, by definition, $n = \rho_i / 2\pi d$ and

$$\rho_i = 2\pi n d. \qquad (8)$$

Siegenbeek van Heukelom et al. (1972) derived the following equation (in equivalent terms from this paper):

$$\rho_i = \rho_c + R_j / l 3^{1/2} \qquad (9)$$

(their Eq. 17). This equation can be expressed as

$$\rho_i = \rho_c + R_j / \omega. \qquad (9a)$$

Table 3. Comparison of calculated junctional and nonjunctional resistances for all data sets and treatments

Data set	ρ_i ($10^3\,\Omega$cm)	R_j (Ωcm^2)	r_j ($10^6\,\Omega$)	R_m ($10^4\,\Omega$cm^2)	r_m ($10^8\,\Omega$)
Untransformed:					
AORTIC	6.90	22.2	6.54	1.07	5.81
VEIN	4.64	17.2	6.90	1.24	4.98
ln-Transformed:					
AORTIC	3.91	12.4	3.67	1.13	6.14
VEIN	2.47	9.0	3.60	2.17	8.72

If the junctions are assumed to be continuously distributed around the perimeter of the model hexagonal cell (*see* Discussion), the junctional resistance of a cell should equal the specific resistance (R_j) divided by the area involved or

$$r_j = R_j/6ld. \tag{10}$$

Combining Eq. (9a) and (10):

$$r_j = (\rho_i - \rho_c)\,3^{1/2}/6d. \tag{11}$$

In the case of the AORTIC data set (ln-transformed), if $\rho_c = 100$ Ωcm (a common value from the literature; *see* Schanne, 1969), $\rho_i = 3.91 \times 10^3$ Ωcm and $d = 3.0 \times 10^{-4}$ cm, then $r_j = 3.67 \times 10^6$ Ω. This value for r_j represents the parallel resistances of 6 interfaces between adjacent cells. If the resistance is expressed per interface

$$r_{j,l} = 6r_j = (\rho_i - \rho_c)\,3^{1/2}/d \tag{12}$$

and, in the above example, $r_{j,l} = 2.20 \times 10^7$ Ω.

Calculated values for ρ_i, R_j and r_j for each of the data sets and treatments are listed in Table 3.

Nonjunctional Resistance. In the original formulations of the thin-sheet model (i.e., Jongsma & Van Rijn, 1972), the space constant was defined as

$$\lambda = (R_m d/2\rho_i)^{1/2}. \tag{13}$$

Solving for the specific nonjunctional resistance,

$$R_m = 2\rho_i \lambda^2/d. \tag{13a}$$

Combining Eqs. (8) and (13a),

$$R_m = 4\pi n \lambda^2. \tag{14}$$

In the absence of detailed information on the comparative specific resistances and areas of the upper and lower membrane surfaces, it was assumed that both contributed equally. Therefore, the nonjunctional resistance of an average cell was simply obtained from the planar surface area and the specific resistance:

$$r_m = R_m/2(1.5\,l^2 \cot 30°) = R_m/1.732\,\omega^2. \tag{15}$$

The estimates for R_m and r_m for the different data sets and treatments are listed in Table 3.

Discussion

The detection of steady-state potential deflections in monolayer cells consequent to injection of current into other cells is indicative of relatively low resistance pathways between the cells and is most reasonably explained by junctional transfer. The possibility that our results might be artifactual can be fairly easily dismissed since we have shown in the same cells that the fluorescent dye, Lucifer yellow CH, passes from cell to cell without detectable leakage to the extracellular space (Larson & Sheridan, 1982). While cytoplasmic bridges may occur, they are unlikely to be common in slowly growing cultures and, moreover, would produce apparent junctional resistances orders of magnitude lower than those we obtained. Therefore, it is reasonable to conclude that we have demonstrated widespread junctional transfer in our cultures of endothelial cells.

The basic physical assumptions inherent in the thin-sheet model are: 1) The monolayer is assumed to consist of parallel upper and lower planar leaky insulators enclosing a uniform conducting fluid; 2) the radial extent of the monolayer is assumed to be infinite in relation to the thickness; 3) current is assumed to flow in two directions only, radially and at right angles across the planar insulators; and 4) junctional resistances between cells are assumed to

be constant throughout the cultures and low enough that the fall-off of induced potential does not show sharp discontinuities at junctional interfaces.

Assumptions 1 and 2 primarily deal with the same problem expressed in assumption 3, current flow in only two directions. At extremely short distances ($r \leqq d$), current can be expected to flow in all directions spherically from a small source. Corrections for short distances (Eisenberg & Johnson, 1970) were not needed in this study, however, as the smallest interelectrode distance was several times the thickness of the monolayer (and the corresponding corrections would have been insignificant). Beyond local effects, the electrode can be assumed to be a cylindrical source with a height equal to d. Since the actual extent of the monolayer in a 60-mm dish was hundreds of times greater than the space constants, the monolayers could be assumed to be infinite relative to the thicknesses.

Since the monolayers used in this study were very uniform in packing density and cell distribution, a major deviation from the above assumptions was in the physical structure of individual cells and particularly in the variable cell thicknesses. The significant parameter in this regard, the electrically effective thickness, must lie somewhere between the maximum cell thickness (perinuclear) and the minimum (the cell height at junctional contact points).

In the absence of an independent measurement of the electrically effective thickness, the estimates listed in Table 1 were used. It is clear, because of the uncertainties in these values, that less weight should be given to calculated parameters that are directly proportional to thickness, i.e. ρ_i, R_j, etc.

On the other hand, the precise value of d had less effect on estimates of r_j and R_m or r_m since, in these cases, the thickness term was partially cancelled out in Eqs. (11) and (13a) ($\rho_i = 2\pi n d$). An order of magnitude reduction in d produced only a 13% reduction in r_j (Eq. 11).

We have no direct way to evaluate the constancy of junctional resistances (first part of assumption 4), although dye injection experiments (Larson & Sheridan, 1982) indicate some variability. We can, however, address the second part of assumption 4. Despite the large difference between the presumed cytoplasmic (ρ_c) and calculated junctional ($\rho_i - \rho_c$) resistivities, the use of a continuous rather than a discontinuous model was justified through reference to Siegenbeek van Heukelom et al. (1972)[2] who found virtual identity between the two models when $\Delta = 2.6\ (l/d)(R_j/R_m) = r_{j,l}/r_m = 0.0301$. Comparisons were not reported for other values of delta. All of our data sets and treatments yield deltas that were in this range (0.068 to 0.025).

Since the least-squares analysis requires homoscedasticity of variances, a natural-logarithmic transformation was carried out on the separate data sets and equations. This treatment gave a better apparent adherence to the above assumption, as can be seen in Fig. 4, without disturbing the theoretical bases of the equations. The effect of this transformation was to uniformly reduce the junctional and increase the nonjunctional resistance estimates (Table 3). Based on the above reasoning, these values should be more representative of the actual cellular resistances. Therefore, our best estimates of junctional resistance (r_j) for the aortic and umbilical vein endothelial cells are 3.67 and $3.60 \times 10^6\ \Omega$, respectively, and those for the nonjunctional resistance (r_m) are 6.14 and $8.72 \times 10^8\ \Omega$ (Table 3).

An estimate of the minimal number of gap junction particles (P) required for these junctional resistances can be made using an upper limit value for individual channel conductance. The junctional resistance can be expressed as a conductance ($g_j = 1/r_j$) which is composed of six parallel equivalent conductances ($g_{j,l}$) corresponding to the six interfaces per cell (*see above*). In the case of the ln-transformed AORTIC data set, $g_j = 2.72 \times 10^{-7}$ mho and, since parallel conductances are additive, $g_{j,l} = 4.54 \times 10^{-8}$ mho. If it is assumed that all particles in the gap junctions are electrically equivalent, then they should each have the same conductance ($g_{j,i}$). The upper-limit estimate for this single-channel conductance is 10^{-10} mho (Loewenstein, 1976; Sheridan et al., 1978). All of the particle conductances are parallel so $g_{j,l}/g_{j,i} = P \simeq 454$ for the aortic and 463 for the umbilical vein cells. These lower-limit values for the number of junctional channels per interface are quite reasonable based on observations of freeze-fracture replicas (Larson & Sheridan, 1982).

In order to provide a comparison of electrical coupling in aortic and venous endothelial

[2] In their original formulation, $\Delta = 0.015$. Since these authors did not include the lower membrane surface in their calculation of R_m, the specific nonjunctional resistances were underestimated by a factor of two (approximately). Therefore, the reported delta value has been doubled to compensate.

Table 4. Variability of the estimates of r_j and r_m due to the variability of n, λ, d and ω for all data sets and treatments

Data set	$r_j \pm$SD ($10^6\ \Omega$)	$r_m \pm$SD ($10^8\ \Omega$)
Untransformed:		
AORTIC	6.54 ± 1.20	5.81 ± 2.98
VEIN	6.90 ± 1.23	4.98 ± 4.12
ln-Transformed:		
AORTIC	3.67 ± 0.46	6.14 ± 3.61
VEIN	3.60 ± 0.45	8.72 ± 7.08

cultures, it was necessary to analyze the statistical fit of the experimental data to the theoretical equations (Eqs. (20) and (4)). Explanations of the statistical analyses are given in the accompanying Appendix. The use of a modified maximum likelihood test gave variances for the estimates of n and λ (Table 2). These variances, combined with those for the estimates of d, allowed the calculation of the variances of the estimates of the resistance parameters (Table 4) by the method of propagation of errors. With these variances, comparisons were made, by hypothesis testing, between the estimated resistances for the aortic and venous cells. It can be assumed that the estimates (ξ) come from normally distributed populations with variances (V) equal to the variances derived above (*see* Appendix). The appropriate test statistic is

$$Z = (\xi_1 - \xi_2)/(V_1 - V_2)^{1/2}. \tag{16}$$

Examination of the specific values of r_j and r_m from Table 4 reveals no statistically significant differences between aortic and umbilical vein cells ($z < z_{0.89}$). This conclusion is not surprising due to the large variabilities of the initial estimated parameters (n and λ; Table 2) and the relationship noted in the Appendix (Fig. A1). In addition, the lack of any clearly defined difference in junctional size between the two cell types (Larson & Sheridan, 1982) suggests that these cells behave similarly in culture, at least with respect to electrotonic transfer characteristics.

Finally, a few comments should be made regarding the usefulness of this electrophysiological analysis for comparing the capabilities for junctional communication in different populations of cultured endothelial cells.

1) First, because of the variability of data points even after ln-transformation, only rather large differences in λ and n will be distinguishable statistically. Nevertheless, this method is superior to others (e.g. determination of coupling coefficient) because the relative contributions of junctional and nonjunctional resistances to λ and n can be assessed.

2) As long as the junctional channels act as passive diffusion pathways, changes in junctional electrical conductance implies a change in junctional permeability to larger molecules. These changes will be strictly proportional if based on changes in the number of open channels, i.e. due either to changes in junctional area or to all-or-none closure or opening of existing channels. Strict proportionality would not be expected, however, if there were partial closing or opening of channels with the greatest discrepancies being for molecules approaching the diameter of the fully open channel and/or having large charge. It is even possible to have a difference in permeability to large molecules without a significant difference in electrical conductance. Thus, direct measurement with molecular probes, e.g. dyes, is advisible (Larson & Sheridan, 1982).

3) Changes in electrical conductance (or even electrical coupling) *per se* might have a functional significance if there are important cell processes directly dependent on the transfer of small ions and/or electrical potential changes. It has been shown, for example, that endothelial cells are hyperpolarized by ACh (Venter et al., 1975). Gap junctions might serve to distribute such potential changes, or the ions producing the changes, throughout the cell population (similar homeostatic roles for junctional communication have been suggested by *several authors;* e.g. Loewenstein, 1976). If so, the degree of electrical coupling and/or magnitude of junctional conductance would be direct measures of the capability for this form of communication.

The authors are grateful to Ms. Patricia Anaya and Ms. Susan Anderson for their excellent technical assistance on this project and to Ms. Jean Borrett who painstakingly typed the manuscript. Dr. Eugene Johnson provided invaluable consultation during the development of the statistical analyses. This work was supported by N.I.H. grants HL 06314 and HL 21166.

Appendix

Statistical Analyses of Fitting and Estimation Procedures for the Thin Sheet Model for Current Flow

Scant attention has been given, in the literature, to statistical analysis of the fitting procedure outlined in the forego-

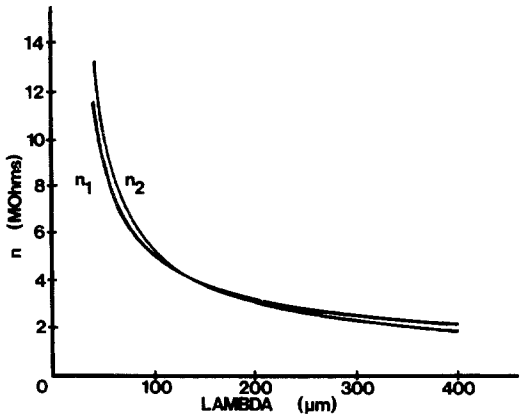

Fig. A1. Plots of n_1 and n_2 (MΩ) from the first partial differentials of Eq. (3) over a range of values for λ (micrometers) for the untransformed data set AORTIC. The single intersection point (152.5, 3.66) provides the best estimates of λ and n

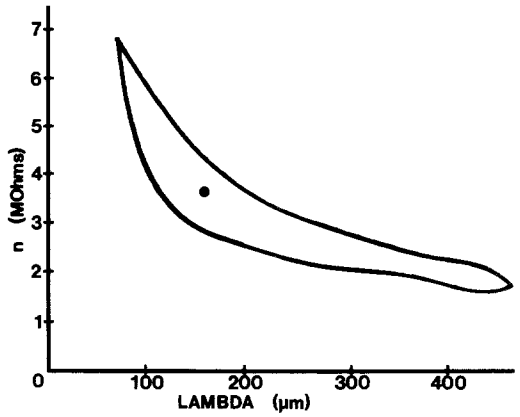

Fig. A2. Approximate 95% confidence contour for the best estimates of λ and n for the untransformed data set AORTIC. The indicated point (152.5, 3.66) represents the smallest value for S (Eq. 3)

ing paper. While it can be assumed that the derived n's and λ's define the best fitting solutions to Eqs. (2) and (4) under the assumptions employed (especially after using the logarithmic transformation), it is not obvious or simple to determine the reliability of these estimates.

Analysis of the Fitting Procedure

Jongsma and van Rijn (1972) defined a test statistic which tests the correspondence of the data with the experimental model equation. While their general equation can be used to make comparisons between different data sets or models, it gives no direct information on the accuracy of estimates of n and λ. Since these parameters are used for estimation of the resistance terms from the model, the reliability of estimates of r_j and r_m depend upon the reliability of estimates of n and λ.

A more useful statistical method was derived by utilizing the maximum likelihood test for goodness of fit (e.g., Beck & Arnold, 1977). The particular modification used was as follows.

The second partial differentials based on Eqs. (3) or (5)[1] were derived ($\delta^2 S^*/\delta n^2$; $\delta^2 S^*/\delta n\,\delta\lambda$; $\delta^2 S^*/\delta\lambda^2$; rules for differentiating Bessel functions are given in Abramowitz and Stegun, 1964). These expressions were set up in a 2×2 matrix, inverted, and multiplied by the sum of squares (S^*; Eq. 5) divided by the number of degrees of freedom ($X-2$). The resulting values for the different data sets constitute the variance/covariance matricies for the estimated parameters based on the fit with the theoretical equation (Eq. 5). These solutions are presented in Table 2 (as the standard deviations $=V^{1/2}$) along with those from the corresponding analyses based on Eq. (3).

[1] The following analysis is based on Eq. (5). The corresponding analysis for Eq. (3) is strictly parallel and is not presented.

Effects of the Variability of the Estimates of n and λ on the Calculated Values of r_j and r_m

The estimates of r_j, found in Table 3, were calculated from Eq. (11) by using the calculated value of ρ_i, the assumed value of $\rho_c=100$ Ωcm and the estimated value of d for each data set (Table 1). Since $\rho_i=2\pi nd$, Eq. (11) can also be expressed as

$$r_j=1.8138\,n-28.8675\,d^{-1}. \tag{A1}$$

Similarly, since $R_m=4\pi n\lambda$ (Eq. 14), the calculating equation for r_m (Eq. 15) can be rewritten as

$$r_m=7.2550\,n\lambda^2\omega^{-2}. \tag{A2}$$

In both of these expressions, the estimated values of n, λ, d and $\omega(\xi(n)$, etc.) were used for each separate data set. Clearly, the variability of the calculated values of r_j and r_m depends upon the variability and covariability of the component parameters. In order to calculate the variances of the junctional and nonjunctional resistance estimates, the general procedure of propagation of errors was employed (e.g., Bevington, 1969).

The basic expression for the variance ($V(x)$) of a function $x=f(u,v,\ldots)$, where $u, v, \ldots$ are variables, is

$$V(x)\simeq V(u)(\delta x/\delta u)^2+V(v)(\delta x/\delta v)^2 +2\,\mathrm{cov}(u,v)(\delta x/\delta u)(\delta x/\delta v)+\ldots. \tag{A3}$$

For the sake of simplicity, this expression neglects the higher order components of the Taylor's expansion.

In the case of Eq. (A1), where $r_j=f(n,d)$, this general expression becomes

$$V(r_j)\simeq V(n)(\delta r_j/\delta n)^2+V(d)(\delta r_j/\delta d)^2 +2\,\mathrm{cov}(n,d)(\delta r_j/\delta n)(\delta r_j/\delta d). \tag{A4}$$

While n and d are certainly related by several equations, there is no reason to suppose that the errors of the estimates of n and d are related. Therefore, cov (n, d) was set equal to zero and the third term of Eq. (A4) dropped out. Since $\delta r_j/\delta n = 1.8138$ and $\delta r_j/\delta d = 28.8675\, d^{-2}$,

$$V(r_j) \simeq V(n)(3.28987) + V(d)(833.333\, \xi^{-4}(d)) \qquad (A5)$$

(where $\xi(d)$ is the estimated value of d for the cell type in question).

The expression of Eq. (A3) for the nonjunctional resistance is strictly parallel but more complicated since $r_m = f(n, \lambda, \omega)$. However, since cov (n, ω) and cov (λ, ω) can be assumed to be zero, the solution is considerably simplified.

The calculated $V(n)$, $V(\lambda)$, $V(d)$, $V(\omega)$ and cov (n, λ) and the estimated (ξ) values of n, λ, d and ω^* were used to calculate $V(r_j)$ and $V(r_m)$ for each data set. The variabilities of r_j and r_m are presented in Table 4 as the estimated values of r_j and r_m from Table 3 plus or minus their standard deviations $(V^{1/2})$.

Explanation of the Variability of the Estimates of n and λ

The individual and joint variability of n and λ (Table 2) can be explained by reference to Figs. A1 and A2. These plots show the relationships of n and λ for the untransformed data set AORTIC. Figure A1 shows the calculated values for n_1 and n_2 (from the first partial differentials of Eq. 3) over a range of values for λ (Jongsma & van Rijn, 1972). It is clear that these functions converge slowly when close to the best λ and n, that is, the point of intersection (152.5, 3.66).

Another way to describe the close relationship of n and λ is demonstrated in Fig. A2. The set of all possible values for S (Eq. 3) would constitute a curved surface above the $\lambda \times n$ plane in a three-dimensional plot. The minimum value for S (and the best λ and n) is the designated point (152.5, 3.66): this point corresponds to the closest approach of the S surface to the $\lambda \times n$ plane. In order to illustrate the relationship of n and λ to this surface, a confidence contour based on the F-test was calculated (*see* Beck & Arnold, 1977). The confidence contour[2] shown in Fig. A2 is the exact projection of the values of S which can be assigned an approximate 95% confidence level (the approximation is due to the nonlinearity of the model equation, the contour is exact).

There are clearly a wide variety of n and λ values which fit the AORTIC data set as well (statistically) as do the derived best n and λ. The relative height and length of the ellipsoidal area demonstrate the variability of n *and* λ and were roughly the same in this example (when allowance was made for the different scales). The slope of the major axis and the width of the area demonstrate the correlation and covariability of n and λ. While the area within the confidence contour is dependent upon the data, the existence of the relationship is inherent in the equations defining S, n and λ.

[2] The curves depicted in Fig. A2 were fit using a least-squares analysis to find two polynomials (upper and lower curves). Each equation was limited to a 6 degree fit.

References

Abramowitz, M., Stegun, I.A. 1964. Handbook of Mathematical Functions. National Bureau of Standards, Washington, D.C.

Amos, D.E., Daniel, S.L. 1975. CDC 6600 subroutines for Bessel functions. Sandia Laboratories (SAND 75-0149)

Beck, J.V., Arnold, K.J. 1977. Parameter Estimation in Engineering and Science. John Wiley and Sons, Inc., New York

Bevington, P.R. 1969. Data Reduction and Error Analysis for the Physical Sciences. McGraw-Hill, New York

Booyse, F.M., Sedlak, B.J., Rafelson, M.E., Jr. 1975. Culture of arterial endothelial cells. *Thromb. Diath. Haemorrh.* **34**:825–839

Buonassisi, V., Colburn, P. 1980. Hormone and surface receptors in vascular endothelium. *In:* advances in Microcirculation. B.M. Altura, editor. Vol. 9, pp. 76–94. S. Karger, Basel

Buonassisi, V., Venter, J.C. 1976. Hormone and neurotransmitter receptors in an established vascular endothelial cell line. *Proc. Natl. Acad. Sci. USA* **73**:1612–1616

D'Amore, P., Shepro, D. 1977. Stimulation of growth and calcium influx in cultured, bovine, aortic endothelial cells by platelets and vasoactive substances. *J. Cell. Physiol.* **92**:177–183

Eisenberg, R.S., Johnson, E.A. 1970. Three-dimensional electrical field problems in physiology. *Prog. Biophys. Mol. Biol.* **20**:1–65

Gimbrone, M.A., Jr. 1976. Culture of vascular endothelium. *In:* Progress in Hemostasis and Thrombosis. T.H. Spaet, editor. Vol. III, pp. 1–28. Grune & Stratton, New York

Gimbrone, M.A., Jr., Cotran, R.S., Folkman, J. 1974. Human vascular endothelial cells in culture. Growth and DNA synthesis. *J. Cell Biol.* **60**:673–684

Haudenschild, C.C., Cotran, R.S., Gimbrone, M.A., Jr., Folkman, J. 1975. Fine structure of vascular endothelium in culture. *J. Ultrastruct. Res.* **50**:22–32

Hooper, M.L., Subak-Sharpe, J.H. 1981. Metabolic cooperation between cells. *Int. Rev. Cytol.* **69**:45–104

Hyde, A., Blondel, B., Matter, A., Cheneval, J.P., Filloux, B., Girardier, L. 1969. Homo- and heterocellular junctions in cell cultures: An electrophysiological and morphological study. *In:* Progress in Brain Research. K. Akert and P.G. Waser, editors. Vol. 31, pp. 283–311. Elsevier Publishing Co., Amsterdam

Jaffe, E.A., Hoyer, L.W., Nachman, R.L. 1973. Synthesis of anti-hemophilic factor antigen by cultured human endothelial cells. *J. Clin. Invest.* **52**:2757–2764

Jongsma, H.J., Rijn, H.E. van 1972. Electronic spread of current in monolayer cultures of neonatal rat heart cells. *J. Membrane Biol.* **9**:341–360

Larson, D.M. 1980. Junctional Transfer of Small Molecules in Cultured Vascular Endothelium. Ph.D. Thesis, University of Minnesota, Minneapolis

Larson, D.M., Sheridan, J.D. 1979. Structure of gap and tight junctions and transfer of small molecules from cell to cell in cultured bovine endothelial cells. *Anat. Rec.* **193**:599 (*Abs*).

Larson, D.M., Sheridan, J.D. 1982. Intercellular junctions and transfer of small molecules in primary vascular endothelial cultures. *J. Cell Biol.* **92**:183–191

Loewenstein, W.R. 1976. Permeable junctions. *Cold Spring Harbor Symp. Quant. Biol.* **40**:49–63

Macarak, E.J., Howard, B.V., Kefalides, N.A. 1977. Pro-

perties of calf endothelial cells in culture. *Lab. Invest.* **36**:62–67

Mason, R.G., Mohammad, S.F., Saba, H.I., Chuang, H.Y.K., Lee, E.L., Balis, J.U. 1979. Functions of endothelium. *In:* Pathobiology Annual 1979, Vol. 9

McNutt, N.S., Weinstein, R.S. 1973. Membrane ultrastructure at mammalian intercellular junctions. *Prog. Biophys. Mol. Biol.* **26**:45–101

Ryan, U.S., Clements, E., Habliston, D., Ryan, J.W. 1978. Isolation and culture of pulmonary artery endothelial cells. *Tissue Cell* **10**:535–554

Schanne, O. 1969. Measurement of cytoplasmic resistivity by means of the glass microelectrode. *In:* Glass Microelectrodes. M. Lavallée, O.F. Schanne, and N.C. Hébert, editors. pp. 299–321. John Wiley and Sons, New York

Schmidt, M.J. 1975. Understanding and Using Statistics: Basic Concepts. D.C. Heath and Co., Lexington, Mass.

Schwartz, S.M. 1978. Selection and characterization of bovine aortic endothelial cells. *In Vitro* **14**:966–980

Sheridan, J.D., Hammer-Wilson, M., Preus, D., Johnson, R.G. 1978. Quantitative analysis of low-resistance junctions between cultured cells and correlation with gap junctional areas. *J. Cell Biol.* **76**:532–544

Shiba, H. 1971. Heaviside's "Bessel cable" as an electric model for flat simple epithelial cells with low resistive junctional membranes. *J. Theoret. Biol.* **30**:59–68

Shiba, H., Kanno, Y. 1971. Further study of the two-dimensional cable theory: An electrical model for a flat thin association of cells with a directional intercellular communication. *Biophysik* **7**:295–301

Siegenbeek van Heukelom, J., Denier van der Gon, J.J., Prop, F.J.A. 1972. Model approaches for evaluation of cell coupling in monolayers. *J. Membrane Biol.* **7**:88–110

Simionescu, N., Simionescu, M. 1977. The cardiovascular system. *In:* Histology, 4th Edition. L. Weiss and R.O. Greep, editors. pp. 373–431. McGraw-Hill Book Co., New York

Simionescu, M., Simionescu, N., Palade, G.E. 1975. Segmental differentiations of cell junctions in the vascular endothelium: The microvasculature. *J. Cell Biol.* **67**:863–885

Simionescu, M., Simionescu, N., Palade, G.E. 1976. Segmental differentiations of cell junctions in the vascular endothelium: Arteries and veins. *J. Cell Biol.* **68**:705–723

Tasaki, K., Tsukahara, Y., Ito, S., Wayner, M.J., Yu, W.Y. 1968. A simple direct and rapid method for filling microelectrodes. *Physiol. Behav.* **3**:1009–1010

Venter, J.C., Buonassisi, V., Bevan, S., Heinemann, S., Bevan, J.A. 1975. Hormone and neurotransmitter receptors on the intimal endothelium. *Blood Vessels* **12**:381–382

Woodbury, J.W., Crill, W.E. 1961. On the problem of impulse conduction in the atrium. *In:* Nervous Inhibition. Proc. Second Friday Harbor Symp. pp. 124–135. Pergammon Press, New York

Received 20 July 1982; revised 10 January 1983